3

Rank M-type Filters for Image Denoising

Francisco J. Gallegos-Funes and Alberto J. Rosales-Silva
National Polytechnic Institute of Mexico
Mexico

1. Introduction

Many different classes of filters have been proposed for removing noise from images (Astola & Kuosmanen, 1997; Bovik, 2000; Kotropoulos & Pitas, 2001). They are classified into several categories depending on specific applications. Linear filters are efficient for Gaussian noise removal but often distort edges and have poor performance against impulsive noise. Nonlinear filters are designed to suppress noise of different nature, they can remove impulsive noise and guarantee detail preservation. Rank order based filters have received considerable attention due to their inherent outlier rejection and detail preservation properties.

In the last decade, many useful techniques of multichannel signal processing based on vector processing have been investigated due to the inherent correlation that exists between the image channels compared to traditional component-wise approaches. Many applications of this technique are color image processing, remote sensing, robot vision, biomedical image processing, and high-definition television (HDTV). Different filtering techniques have been proposed for color imaging (Plataniotis & Venetsanopoulos, 2000). Particularly, nonlinear filters applied to color images have been designed to preserve edges and details, and remove impulsive noise. On the other hand, the filters based in the wavelet domain provide a better performance in terms of noise suppression in comparison with different spatial domain filters (Mahbubur Rahman & Kamrul Hasan, 2003).

The possibility to process 3D images presents a new application where it is necessary to improve the quality of 3D objects inside the image, suppressing a noise of different nature (impulsive, Gaussian noise, or may be by speckle one) that always affects the communication or acquisition process (Nikolaidis & Pitas, 2001). Multiplicative (speckle) noise is common for any system using a coherent sensor, for example, the ultrasound transducer. Other problem that is not trivial is the adaptation and implementation of the current filters, that have been investigated in different papers in the case of 2D image processing to process objects in 3D by use multiframe methods to increase the signal-to-noise ratio (SNR).

This chapter presents the capability features of robust Rank M-Type K-Nearest Neighbor (RMKNN) and Median M-Type L- (MML) filters for the removal of impulsive noise in gray-scale image processing applications (Gallegos & Ponomaryov, 2004; Gallegos-Funes et al., 2005; Gallegos-Funes et al., 2008). The proposed scheme is based on combined robust *R*- (median, Wilcoxon, Ansari-Bradley-Siegel-Tukey or Mood) and *M*-estimators, and modification of the KNN and L- filters that use the RM (Rank M-type) -estimator to calculate

Source: Image Processing, Book edited by: Yung-Sheng Chen,
ISBN 978-953-307-026-1, pp. 572, December 2009, INTECH, Croatia, downloaded from SCIYO.COM

the robust point estimate of the pixels within the filtering window. So, such filters use the value of the central pixel within the filtering window to provide the preservation of fine details and the redescending *M*-estimators combined with the calculation of the rank estimator to obtain the sufficient impulsive noise rejection. Different types of influence functions in the *M*-estimator can be used to provide better impulsive noise suppression. We apply the proposed MML filter in SAR images which naturally have speckle noise to demonstrate that the speckle noise can be efficiently suppressed, while the sharpness and fine feature are preserved.

The robust Rank M-Type K-Nearest Neighbor (RMKNN) filters are adapted to work in color image denoising (Ponomaryov et al., 2005). We also present the 3D RMKNN and 3D MML filters which are compared with different nonlinear 2D filters which were adapted to 3D (Varela-Benitez et al., 2007a). The experimental results were realized by degraded an ultrasound sequence with different variance of speckle noise added to the natural speckle noise of the sequence. Finally, we adapt the RMKNN, MML, and different order statistics filters to work in the wavelet domain for the removal of impulsive and speckle noise in gray-scale and color image processing applications (Gallegos-Funes et al., 2007; Varela-Benitez et al., 2007b).

Another goal of this chapter is to demonstrate the possibility to implement the filters in order to process the image or sequence in real time by means of use of the Texas Instruments DSP TMS320C6701 and DSP TMS320C6711 to demonstrate that the proposed methods potentially could provide a real-time solution to quality video transmission.

Extensive simulation results with different gray scale and color images and video sequences have demonstrated that the proposed filters consistently outperform other filters by balancing the tradeoff between noise suppression, fine detail preservation, and color retention.

2. Rank M-type estimators

2.1 R-estimators

The *R*-estimators are a class of nonparametric robust estimators based on rank calculations (Hampel et al., 1986; Huber, 1981). We consider a two-samples of rank tests $x_1,\ldots,x_m$ and $y_1,\ldots,y_n$ as a two-samples with distributions $H(x)$ and $H(x+\Delta)$, where Δ is the shift of unknown location. Let $X_{(i)}$ be the rank of X_i in the pooled sample of size $N=m+n$. The rank test of $\Delta=0$ against $\Delta>0$ is based on the statistics test,

$$S=\frac{1}{m}\sum_{i=1}^{m}a_i\left(X_{(i)}\right) \tag{1}$$

Usually, the scores a_i are generated by the function J as follows:

$$a_i=N\int_{(i-1)/N}^{i/N}J(t)dt \tag{2}$$

The function $J(t)$ is symmetric in the sense of $J(1-t)=-J(t)$, satisfies $\int J(t)dt=0$ and the coefficients a_i are given as $\sum_{i=1}^{n}a_i=0$.

The median estimator can be derived from Laplace distribution function $f_0(x)=\frac{1}{2}e^{-|x|}$ with function $J(t)=\begin{cases}-1 & t<\frac{1}{2}\\ 1 & t>\frac{1}{2}\end{cases}$ and is given in such a form (Hampel et al., 1986; Huber, 1981):

$$\hat{\theta}_{\text{med}}=\begin{cases}\frac{1}{2}\left(X_{(n/2)}+X_{(1+n/2)}\right), & \text{for even } n\\ X_{\left(\frac{n+1}{2}\right)}, & \text{for odd } n\end{cases} \tag{3}$$

where $X_{(j)}$ is the element with rank j. It is the best estimator when any *a priori* information about data X_i distribution shape and its moments is unavailable.

The Hodges-Lehmann estimator $J(t)=\left|t-\frac{1}{2}\right|$ is relational with Wilcoxon test and logistic distribution function $f_0(x)=\frac{1}{1+e^{-x}}$. The corresponding rank estimator is the Wilcoxon *R*-estimator (Hampel et al., 1986; Huber, 1981):

$$\hat{\theta}_{\text{Wil}}=\underset{i\le j}{\text{MED}}\left\{\frac{1}{2}\left(X_{(i)}+X_{(j)}\right),\ i,j=1,\dots N\right\} \tag{4}$$

The Wilcoxon estimator is robust and unbiased. When the shape of the original data distribution is symmetrical, the such a test is known as the local asymptotically most powerful one.

Other *R*-estimations can be obtained by different type of functions $J(t)$. For example, the functions Ansari-Bradley-Siegel-Tukey $J(t)=\left|t-\frac{1}{2}\right|-\frac{1}{4}$ and Mood $J(t)=\left(t-\frac{1}{2}\right)^2-\frac{1}{12}$ determine the *R*-estimators (Hampel et al., 1986; Huber, 1981):

$$\hat{\theta}_{\text{ABST}}=\text{MED}\left\{\begin{matrix}X_{(i)} & , & i\le\left[\frac{N}{2}\right]\\ \frac{1}{2}\left(X_{(i)}+X_{(j)}\right), & & \left[\frac{N}{2}\right]<i\le N\end{matrix}\right\} \tag{5}$$

$$\hat{\theta}_{\text{MOOD}}=\text{MED}\left\{\begin{matrix}\frac{1}{2}\left(X_{(i)}+X_{(j)}\right), & i\le 3\\ X_{(i)} & , & 3<i\le N\end{matrix}\right\} \tag{6}$$

2.2 M-estimators

The *M*-estimators are a generalization of maximum likelihood estimators (MLE) (Hampel et al., 1986; Huber, 1981). Their definition is given by a function ρ $\{\rho(X)=\ln(F(X))\}$ connected with the probability density function $F(X)$ of data samples X_i, $i=1,\dots,N$:

$$\hat{\theta} = \arg\min_{\theta \in \Theta} \sum_{i=1}^{N} \rho(X_i - \theta) \tag{7}$$

The estimation of the location parameter θ can be found by calculating the partial derivative of ρ (with respect to θ) introducing the function $\psi(X,\theta) = \frac{\partial}{\partial\theta}\rho(X,\theta)$

$$\sum_{i=1}^{N} \psi(X_i - \theta) = 0 \tag{8}$$

where θ is a location parameter.
The robust *M*-estimator solution for θ is determined by imposing certain restrictions on the influence function $\psi(X)$ or the samples $X_i - \theta$, called censorization or trimming. The standard technique for the *M*-estimator assumes the use of Newton's iterative method that can be simplified by a single-step algorithm to calculate the lowered *M*-estimate of the average θ value (Astola & Kuosmanen, 1997)

$$\theta_{\mathbf{M}} = \frac{\sum_{i=1}^{N} X_i \tilde{\psi}\left(X_i - \mathrm{MED}\{\bar{X}\}\right)}{\sum_{i=1}^{N} 1_{[-r,r]}\left(X_i - \mathrm{MED}\{\bar{X}\}\right)} \tag{9}$$

where $\tilde{\psi}$ is the normalized function ψ: $\psi(X) = X\tilde{\psi}(X)$. It is evident that (9) represents the arithmetic average of $\sum_{i=1}^{n} \psi\left(X_i - \mathrm{MED}\{\bar{\mathbf{X}}\}\right)$, which is evaluated on the interval $[-r, r]$. The parameter *r* is connected with restrictions on the range of $\psi(X)$, for example, as it has been done in case of the simplest Huber's limiter type *M*-estimator for the normal distribution having heavy 'tails' (Huber, 1981)

$$\tilde{\psi}_r(X) = \min(r, \max(X, r)) = [X]_{-r}^{r} \tag{10}$$

Another way to derive the function $\tilde{\psi}(X)$ is to cut the outliers off the primary sample. This leads to the so-called lowered *M*-estimates. Hampel proved that the skipped median is the most robust lowered *M*-estimate (Hampel et al., 1986). Below we also use the simple cut (S) function. There exist also other well known influence functions in the literature. We also use the Hampel´s three part redescending (H), Andrew's sine (A), Tukey biweight (T), and the Bernoulli (B) influence functions (Astola & Kuosmanen, 1997; Hampel et al., 1986). These functions are shown in Table 1.

2.3 RM-estimators

The proposal to enhance the robust properties of *M*-estimators and *R*-estimators by using the *R*-estimates consists of the procedure similar to the median average instead of arithmetic one (Gallegos-Funes et al., 2002; Gallegos & Ponomaryov 2004):

$$\theta_{\text{med}\mathbf{M}} = \text{MED}\left\{X_i \tilde{\psi}\left(X_i - \text{MED}\left\{\bar{\mathbf{X}}\right\}\right), i = 1, \ldots, N\right\} \tag{11}$$

$$\theta_{\text{Wil}\mathbf{M}} = \underset{i \le j}{\text{MED}}\left\{\frac{1}{2}\left[X_i \tilde{\psi}\left(X_i - \text{MED}\left\{\bar{\mathbf{X}}\right\}\right) + X_j \tilde{\psi}\left(X_j - \text{MED}\left\{\bar{\mathbf{X}}\right\}\right)\right], \; i = 1, \ldots, N\right\} \tag{12}$$

Influence function	Formulae
Simple cut (S)	$\psi_{\text{cut}(r)}(X) = X \cdot 1_{[-r,r]}(X) = \begin{cases} X, & \lvert X\rvert \le r \\ 0, & \lvert X\rvert > r \end{cases}.$
Hampel's three part redescending (H)	$\psi_{\alpha,\beta,r}(X) = \begin{cases} X, & 0 \le \lvert X\rvert \le \alpha \\ \alpha \cdot \text{sgn}(X), & \alpha \le \lvert X\rvert \le \beta \\ \alpha \dfrac{r - \lvert X\rvert}{r - \beta}, & \beta \le \lvert X\rvert \le r \\ 0, & r \le \lvert X\rvert \end{cases}$, where $0 < \alpha < \beta < r < \infty.$
Andrew's sine (A)	$\psi_{\sin(r)}(X) = \begin{cases} \sin(X/r), & \lvert X\rvert \le r\pi \\ 0, & \lvert X\rvert > r\pi \end{cases}$
Tukey's biweight (T)	$\psi_{\text{bi}(r)}(X) = \begin{cases} X^2\left(r^2 - X^2\right), & \lvert X\rvert \le r \\ 0, & \lvert X\rvert > r \end{cases}$
Bernoulli (B)	$\psi_{\text{ber}(r)}(X) = X^2\sqrt{r^2 - X^2} \cdot 1_{[-r,r]}(X)$

Table 1. Influence functions used in the filtering scheme to derive the robust redescending *M*-estimators.

Such an estimator is the combined RM-estimator. It should be noted that the RM-estimator (11) is the usual median when the function $\tilde{\psi}$ is represented by eq. (10). If the function $\tilde{\psi}$ is described by the simple cut function, it yields the skipped median. Other new RM-estimators applied below are followed from eqs. (5) and (6) (Gallegos-Funes et al., 2005):

$$\theta_{\text{ABST}\mathbf{M}} = \underset{i \le j}{\text{MED}}\left\{\begin{array}{ll} X_i \tilde{\psi}\left(X_i - \text{MED}\left\{\bar{\mathbf{X}}\right\}\right), & i \le \dfrac{N}{2} \\ \dfrac{1}{2}\left[X_i \tilde{\psi}\left(X_i - \text{MED}\left\{\bar{\mathbf{X}}\right\}\right) + X_j \tilde{\psi}\left(X_j - \text{MED}\left\{\bar{\mathbf{X}}\right\}\right)\right], & \dfrac{N}{2} < i \le N \end{array}\right\} \tag{13}$$

$$\theta_{\text{Mood}\mathbf{M}} = \underset{i \le j}{\text{MED}}\left\{\begin{array}{ll} \dfrac{1}{2}\left[X_i \tilde{\psi}\left(X_i - \text{MED}\left\{\bar{\mathbf{X}}\right\}\right) + X_j \tilde{\psi}\left(X_j - \text{MED}\left\{\bar{\mathbf{X}}\right\}\right)\right], & i \le 3 \\ X_i \tilde{\psi}\left(X_i - \text{MED}\left\{\bar{\mathbf{X}}\right\}\right), & 3 < i \le N \end{array}\right\} \tag{14}$$

It is possible to expect that the robust properties of the RM-estimators can exceed the robust properties of the base *R*- and *M*- estimators. The *R*-estimator provides good properties of impulsive noise suppression and the *M*-estimator uses different influence functions according to the scheme proposed by Huber to provide better robustness, for these reasons it can be expected that the properties of combined RM-estimators could be better in

comparison with *R*- and *M*- estimators (Gallegos-Funes et al., 2002; Gallegos & Ponomaryov 2004).

3. Rank M-type filters

To increase the robustness of standard filters, it is possible to employ different methods known in the robust-estimate theory, for example, the censoring or others (Astola & Kuosmanen, 1997; Peltonen & Kuosmanen, 2001). The known proposal to increase the quality of filtration via the preservation both the edges and small-size details in the image consists of the use of KNN image-filtering algorithm. Other proposal filtering schemes proposed here are the L-filter and the versions of KNN and L filters in wavelet domain.

3.1 Rank M-Type KNN filters

The following representation of the KNN filter is usually used $\theta_{\mathrm{KNN}} = \sum_{i=1}^{n} a_i x_i \Big/ \sum_{i=1}^{n} a_i$ with $a_i = \begin{cases} 1, & \text{if } |x_i - x_c| \le T \\ 0, & \text{otherwise} \end{cases}$, x_c is the central pixel, and T is a threshold (Astola & Kuosmanen, 1997). If the threshold T is chosen to be twice of the standard noise deviation σ, this filter is known as the sigma filter. The KNN filter can be rewritten as $\hat{\theta}_{\mathrm{KNN}}(i,j) = \frac{1}{K} \sum_{m=-L}^{L} \sum_{n=-L}^{L} \psi(x(i+m, j+n)) x(i+m, j+n)$ where $x(i+m, j+n)$ are the pixels in the filter window, $m, n = -L, \ldots, L$, and $\psi(x(i+m, j+n)) = \begin{cases} 1, & \text{if } x(i+m, j+n) \text{ are } K \text{ samples whose values are closest to} \\ & \text{the value of the central sample } x \text{ inside the filter window} \\ 0, & \text{otherwise} \end{cases}$.

To improve the robustness of the KNN filter that can preserve well both the edges and the fine details in absence of noise, we proposed to use the RM-estimator (11) given by $\hat{\theta}_{\mathrm{MMKNN}}(i,j) = \mathrm{MED}\{\hat{\theta}_{\mathrm{KNN}}(i+m, j+n)\}$. So, the iterative Median M-type K-Nearest Neighbor filter can be written as (Gallegos-Funes et al., 2002; Gallegos & Ponomaryov 2004),

$$\hat{\theta}^{(w)}_{\mathrm{MMKNN}}(i,j) = \mathrm{MED}\left\{h^{(w)}(i+m, j+n)\right\} \tag{15}$$

where $h^{(w)}(i+m, j+n)$ is a set of K_{close} values of pixels weighting in accordance with the used $\psi(X)$ influence function within the filter window closest to the estimate obtained at previous step $\hat{\theta}^{(w\text{-}1)}_{\mathrm{MMKNN}}(i,j)$. The initial estimate is $\hat{\theta}^{(0)}_{\mathrm{MMKNN}}(i,j) = x(i,j)$ and $\hat{\theta}^{(w)}_{\mathrm{MMKNN}}(i,j)$ denotes the estimate at the iteration w. $x(i,j)$ is the current or origin pixel contaminated by noise in the filtering window. The filtering window size is $N = (2L+1)^2$ and $m, n = -L, \ldots, L$. The current number of the nearest neighbor pixels K_{close} reflects the local data activity and impulsive noise presence (Gallegos & Ponomaryov 2004),

$$K_{close} = \begin{cases} K_{\min} + aD_S, & (K_{\min} + aD_S) \le K_{\max} \\ K_{\max}, & \text{otherwise} \end{cases} \tag{16}$$

The parameter a controls the filter sensitivity for local data variance to detect the details. $K_{\min}$ is the minimal number of neighbours for noise removal and $K_{\max}$ is the maximal number of neighbours for edge restriction and detail smoothing. D_S is the impulsive detector, and MAD is the median of the absolute deviations from the median (Astola & Kuosmanen, 1997) which are defined as (Gallegos & Ponomaryov 2004):

$$D_S = \frac{\mathrm{MED}\left\{\left|x(i,j) - x(i+m, j+n)\right|\right\}}{\mathrm{MAD}\left\{x(i,j)\right\}} + 0.5\frac{\mathrm{MAD}\left\{x(i,j)\right\}}{\mathrm{MED}\left\{x(i+k, j+l)\right\}} \tag{17}$$

$$\mathrm{MAD}\left\{x(i,j)\right\} = \mathrm{MED}\left\{\left|x(i+m, j+n) - \mathrm{MED}\left\{x(i+k, j+l)\right\}\right|\right\} \tag{18}$$

In our experiments, a 3x3 window (i.e., $m,n = -1,\ldots,1$ and $(2L+1)^2 = 9$) is applied. The algorithm finishes when $\hat{\theta}^{(w)}_{\mathrm{MMKNN}}(i,j) = \hat{\theta}^{(w-1)}_{\mathrm{MMKNN}}(i,j)$. The use of the influence functions mentioned above in the proposed filter (15) could provide good suppression of impulsive noise. We also propose for enhancement of the removal ability of MMKNN filter in the presence of impulsive noise to involve the standard median filter. The numerical simulations have shown that for $K_{close} > 7$ the MMKNN filter can be substituted by the *3x3 median* filter and for $K_{close} > 350$ we can use the *5x5 median* filter.

Other versions of Rank M-type K-Nearest Neighbor filters are given as follows (Gallegos-Funes et al., 2005; Ponomaryov et al., 2005),

$$\hat{\theta}^{(w)}_{\mathrm{WMKNN}}(i,j) = \mathrm{MED}\left\{\frac{h^{(w)}(i+m, j+n) + h^{(w)}(i+m_1, j+n_1)}{2}\right\} \tag{19}$$

$$\hat{\theta}^{(w)}_{\mathrm{ABSTMKNN}}(i,j) = \underset{i\le j}{\mathrm{MED}}\left\{\begin{array}{ll} h^{(w)}(i+m.j+n), & i,j \le \dfrac{N}{2} \\ \dfrac{h^{(w)}(i+m, j+n) + h^{(w)}(i+m_1, j+n_1)}{2}, & \dfrac{N}{2} < i \end{array}\right\} \tag{20}$$

$$\hat{\theta}^{(w)}_{\mathrm{MOODMKNN}}(i,j) = \underset{i\le j}{\mathrm{MED}}\left\{\begin{array}{ll} h^{(w)}(i+m.j+n), & 3 < i \le N \\ \dfrac{h^{(w)}(i+m, j+n) + h^{(w)}(i+m_1, j+n_1)}{2}, & i \le 3 \end{array}\right\} \tag{21}$$

3.2 Wavelet domain order statistics filter

This filter constitutes two filters (Gallegos-Funes et al., 2007): the filter based on redundancy of approaches (Gallegos-Funes et al., 2007) and the Wavelet domain Iterative Center Weighted Median (ICWMF) Filter (Mahbubur Rahman & Kamrul Hasan, 2003) as shown in Figure 1. For each color component of the noisy image it is necessary to apply all the steps contained in this structure. This technique applies up to 5 scaling levels for the details and only 1 scaling level for the approaches. Other operations are indicated to make clearer the wavelet analysis that it is carried out in this paper. We modify this structure in the block of the ICWMF. For that reason, the expressions used by the ICWMF to calculate the improved estimation of the variance field of the noisy wavelet coefficients will be required to indicate

when and where different proposed filtering algorithms will take place to improve the performance of the proposed filter.

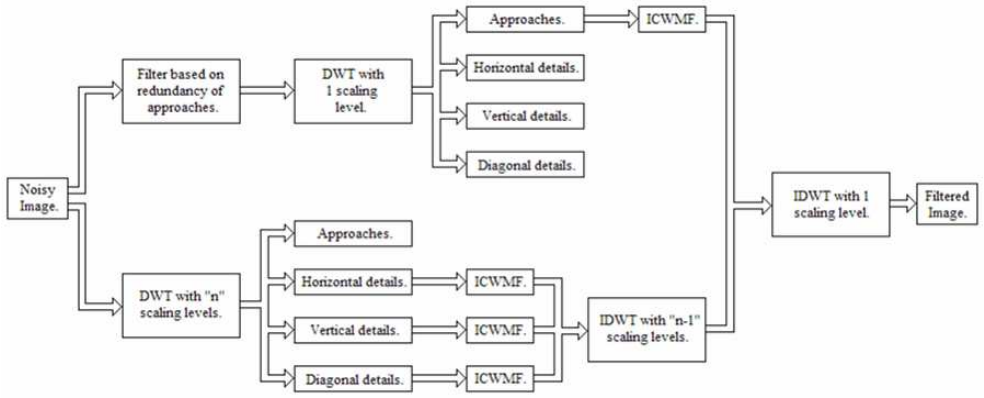

Fig. 1. Block diagram of the proposed filtering scheme of the Wavelet Domain Order Statistics Filter.

The first stage of the ICWMF that detects if a sample contains noise or not is given by:

$$\hat{\sigma}_{gs}^{2}(k)=\begin{cases}\tilde{\sigma}_{gs}^{2}(k), & \text{if } \lambda_s \geq \lambda_{th} \\ med_{cw}^{n}(\tilde{\sigma}_{gs}^{2}(j)), & \text{otherwise}\end{cases} \tag{22}$$

where $\tilde{\sigma}_{gs}^{2}$ is the variance field estimated previously, k is central sample in the filter window, j is one of the N sample contained into the window, λ_s is the standard deviation of the preliminary estimate of the signal coefficients variances $\tilde{\sigma}_{s}^{2}(k)$ in each scale, $\lambda_{th}=\sum_s \lambda_s 2^{-s} / \sum_s 2^{-s}$ is the discriminating threshold, s is the scale used in the wavelet analysis, and 2^{-s} is the weighting function (Mahbubur Rahman & Kamrul Hasan, 2003).

The *Signal dependent rank order mean* (SDROM) (Abreu et al., 1996), *Adaptive Center Weighed Median* (ACWM) (Chen & Wu, 2001), and *Median M-type KNN* (Gallegos-Funes et al., 2007) filters were applied to the proposed filter as a first detection block. But the *FIR Median Hybrid* (FIRMH) filter (Astola & Kuosmanen, 1997) was applied as a second detection block because this algorithm only constitutes the part of estimation of the noisy sample value (only if the sample was detected of this way) and the proposed filter can continue operating in all its sections in the same way. For this reason it is necessary to present the expression for the second detection block contained in the proposed filter structure (Mahbubur Rahman & Kamrul Hasan, 2003):

$$\begin{cases} med\,(\tilde{\sigma}_{gs}^{2}(j)) & \text{if } \tilde{\sigma}_{gs}^{2}(k) \leq \gamma\sigma_{n}^{2} \\ \tilde{\sigma}_{gs}^{2}(k)+med\,(\tilde{\sigma}_{gs}^{2}(j)-\tilde{\sigma}_{gs}^{2}(k)) & \text{otherwise}\end{cases} \tag{23}$$

The proposed filter uses the median algorithm represented as $med(\tilde{\sigma}_{gs}^{2}(j))$ to estimate the value of the central sample in a filter window if the sample is detected as noisy. It is possible

to use other estimation algorithm such as the FIR Median Hybrid Filter that retains more information about the image.

3.3 Median M-type L-filter

We propose to improve the robustness of *L*-filter by means of use of RM-estimator (11). The representation of L-filter is $\theta_{\mathrm{L}} = \sum_{i=1}^{N} a_i \cdot X_{(i)}$ where $X_{(i)}$ is the ordered data sample, i=1,…,N, $a_i = \int_{i-1/N}^{i/N} h(\lambda)d\lambda \Big/ \int_0^1 h(\lambda)d\lambda$ are the weight coefficients, and $h(\lambda)$ is a probability density function (Kotropoulos & Pitas, 2001).

To introduce the MM-estimator (11) in the scheme of *L*-filter, we present the ordered data sample of *L*-filter as function of an influence function (Gallegos-Funes et al., 2008),

$$\hat{\theta}_{\mathrm{L}} = \sum_{i=1}^{N} a_i \cdot \psi(X_i) \cdot X_i \tag{24}$$

where $N=(2L+1)^2$ is the filtering window size, $\psi(X_i)\cdot X_i$ is the ordered data sample, $\psi(u) = \begin{cases} c, & |u| \le r \\ 0, & \text{otherwise} \end{cases}$ is the influence function, c is a constant, and r is connected with the range of $\psi(u)$.

Then, the non iterative MML filter can be obtained by the combination of *L*-filter (24) and the MM-estimator (11) (Gallegos-Funes et al., 2008),

$$\theta_{\mathrm{MML}} = \frac{\mathrm{MED}\left\{a_i \cdot \left[X_i \cdot \psi\left(X_i - \mathrm{MED}\left\{\vec{X}\right\}\right)\right]\right\}}{a_{\mathrm{MED}}} \tag{25}$$

where $X_i \psi\left(X_i - \mathrm{MED}\left\{\vec{X}\right\}\right)$ are the selected pixels in accordance with the influence function used in a sliding filter window, the coefficients a_i are computed using the Laplacian and Uniform distribution functions in $h(\lambda)$, and a_{MED} is the median of coefficients a_i used as a scale constant.

To improve the properties of noise suppression of MML filter we use an impulsive noise detector (IND) (Aizenberg et al., 2003),

$$\mathrm{IND} = \begin{cases} \text{Filtering}, & \text{if } \left[(D \le s) \vee (D \ge N-s)\right] \wedge \left(\left|X_c - \mathrm{MED}\left(\vec{X}\right)\right| \ge U\right) \\ X_c, & \text{otherwise} \end{cases} \tag{26}$$

where X_c is the central pixel in the filtering window, s>0 and U≥0 are thresholds, N is the length of the data, and D=*rank*(X_c) is the rank of element X_c. The expressions $D \le s$ and $D \ge N-s$ come from the fact that the difference between the ranks of the impulse and the median is usually large. In other words, the median is positioned in the center of data, and an impulse is usually positioned near one of its ends. The expression $\left|X_c - \mathrm{MED}\left(\vec{X}\right)\right| \ge U$ has been specially developed for images that have very high corruption rate. Finally, if these conditions are true then we classify X_c as corrupted.

3.4 Wavelet Domain Median M-type L-filter

Figure 2 shows a block diagram of proposed Wavelet Domain Median M-type L (WDMML) filter (Varela-Benitez et al., 2007b). The proposed WDMML filter uses the Daubechie wavelets (Walker, 1999). We apply the proposed MML filter in the gray scale images of approaches and details obtained in the process of wavelet decomposition.

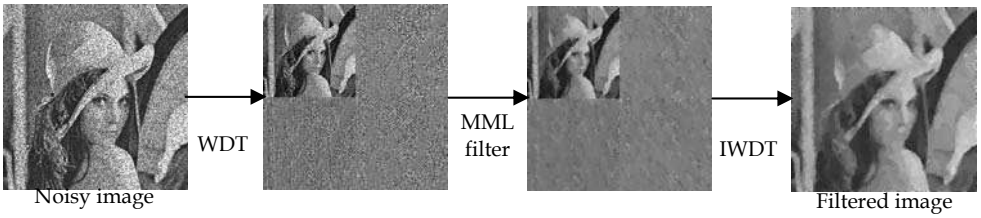

Fig. 2. Block diagram of proposed WDMML filter.

4. Overall filtering performance

The objective criteria used to compare the performance of noise suppression of various filters was the *peak signal to noise ratio* (PSNR) and for the evaluation of fine detail preservation the *mean absolute error* (MAE) was used (Astola & Kuosmanen, 1997; Bovik 2000),

$$\mathrm{PSNR} = 10 \cdot \log\left[\frac{(255)^2}{\mathrm{MSE}}\right] \ \mathrm{dB} \tag{27}$$

$$\mathrm{MAE} = \frac{1}{MN}\sum_{i=0}^{M-1}\sum_{j=0}^{N-1}\left|f(i,j) - \hat{\theta}(i,j)\right| \tag{28}$$

where $\mathrm{MSE} = \frac{1}{MN}\sum_{i=0}^{M-1}\sum_{j=0}^{N-1}\left[f(i,j) - \hat{\theta}(i,j)\right]^2$ is the *mean square error*, $f(i,j)$ is the original image; $\hat{\theta}(i,j)$ is the restored image; and M, N is the size of the image.

In the case of color image processing, we compute the *mean chromaticity error* (MCRE) for evaluation of chromaticity retention, and the *normalized color difference* (NCD) for quantification of color perceptual error (Plataniotis & Venetsanopoulos, 2000):

$$\mathrm{MCRE} = \sum_{i=1}^{M_1}\sum_{j=1}^{M_2}\left\|p_{i,j} - \hat{p}_{i,j}\right\|_{L_2}^2 \Big/ M_1 M_2 \tag{29}$$

$$\mathrm{NCD} = \sum_{i=1}^{M_1}\sum_{j=1}^{M_2}\left\|\Delta E_{Luv}(i,j)\right\|_{L_2} \Big/ \sum_{i=1}^{M_1}\sum_{j=1}^{M_2}\left\|E^*_{Luv}(i,j)\right\|_{L_2} \tag{30}$$

where $p_{i,j}$ and $\hat{p}_{i,j}$ are the intersection points of $f(i,j)$ and $\hat{\theta}(i,j)$ with the plane defined by the Maxwell triangle, respectively, $\left\|\Delta E_{Luv}(i,j)\right\|_{L_2} = \left[\left(\Delta L^*(i,j)\right)^2 + \left(\Delta u^*\right)^2 + \left(\Delta v^*\right)^2\right]^{1/2}$ is the

norm of color error, ΔL^*, Δu^*, and Δv^* are the difference in the L^*, u^*, and v^* components, respectively, between the two color vectors that present the filtered image and uncorrupted original one for each a pixel (i,j) of an image, $\left\| E^*_{Luv}(i,j) \right\|_{L_2} = \left[\left(L^*\right)^2 + \left(u^*\right)^2 + \left(v^*\right)^2 \right]^{1/2}$ is the norm or magnitude of the uncorrupted original image pixel vector in the $L^*u^*v^*$ space, and $\| \ . \ \|_{L_2}$ is the L_2-vector norm.

4.1 Noise suppression in gray scale images and video sequences

The described 3x3 MMKNN, 3x3 WMKNN, 3x3 ABSTMKNN, 3x3 MOODMKNN, and 3x3 MML filters with different influence functions have been evaluated, and their performance has been compared with 3x3 *weighted median* (WM) (Bovik, 2000), 3x3 *tri-state median* (TSM) (Chen et al., 1999), 3x3 *adaptive center weighted median* (ACWM) (Chen & Wu, 2001), 3x3 *rank order mean* (ROM) (Abreu et al., 1996), 3x3 *minimum-maximum exclusive mean* (MMEM) (Wei-Lu & Ja-Chen, 1997), 3x3 *Local Linear Minimum Mean Square Error* (LMMSE) (Özkan et al., 1993), 3x3 *K-Nearest Neighbor* (KNN) (Astola & Kuosmanen, 1997), 3x3 *Ansari-Bradley-Siegel-Tukey* (ABST) (Hampel et al., 1986), 3x3 *Normalized Least Mean Squares L* (NLMS-L) (Kotropoulos & Pitas, 1996), 3x3 *Sampled-Function Weighted Order* (SFWO) (Öten & De Figueiredo, 2002), and *Modified Frost* (MFrost) (Lukin et al., 1998) filters. The reason for choosing these filters to compare them with the proposed ones is that their performances have been compared with various known filters and their advantages have been demonstrated. The runtime analysis of various filters was conducted for different images using Texas Instruments DSP TMS320C6701 (Kehtarnavaz & Keramat, 2001; Texas Instruments, 1998).

To determine the impulsive noise suppression properties of various filters the 256x256 standard test grayscale images "Airfield", "Goldhill", and "Lena" were corrupted with an occurrence rate of 20% of impulsive noise and the results obtained by the mentioned filters are presented in Table 2. One can see from the Table 2 that the proposed MMKNN and WMKNN filters have better performances in terms of PSNR and MAE criteria in comparison with the filters used as comparative in the most of cases. The processing time is given in seconds and includes the duration of data acquisition, processing and storing of data.

The results reveal that the processing time values of the MMKNN filter are larger than WM, and MMEM filters but less in comparison with ACWM, LMMSE, and ROM filters and have about the same values compared to the TSM filter. The MMKNN filter with Andrew's and Bernoulli influence functions take more time than when other influence functions are used depending on the filter parameters values. For the ROM filter the processing time does not include the time for deriving weighting coefficients during the training stage and then used in this filtering scheme. The time used in its training procedure is 0.035 s approximately.

The processing time performance of the MMKNN filter depends on the image to process and almost does not vary for different noise levels; these values also depend on the complex calculation of the influence functions and parameters of the proposed filter. The proposed MMKNN algorithm can process from 16 to 19 images of 256x256 pixels per second. In the case of WMKNN filter we observe that its processing time is larger than MMKNN filter. The WMKNN algorithm can process from 10 to 14 images of 256x256 pixels per second.

In Figure 3 we present the processed images for the test image "Lena" explaining the impulsive noise suppression according to the Table 2. A zoomed-in section (upright) of each image is displayed in order to view the details.

Algorithm	Airfield			Goldhill			Lena		
	PSNR	MAE	TIME	PSNR	MAE		PSNR	MAE	
WM	22.40	10.67	0.0203	24.21	9.96	0.0203	23.58	8.67	0.0203
TSM	21.13	13.44	0.0547	23.11	12.43	0.0547	23.56	10.80	0.0547
ACWM	22.97	10.57	0.2299	24.84	10.43	0.2299	25.56	8.75	0.2299
ROM	23.08	10.42	0.0750	24.82	10.57	0.0750	25.20	9.11	0.0750
MMEM	22.69	12.23	0.0406	24.16	11.09	0.0406	24.52	9.46	0.0406
LMMSE	23.03	11.24	0.0750	24.15	11.08	0.0750	24.59	9.95	0.0751
MMKNN (S)	23.21	10.45	0.0515	25.45	9.58	0.0517	26.38	7.12	0.0515
MMKNN (H)	23.24	10.42	0.0521	25.50	9.50	0.0524	26.33	7.07	0.0521
MMKNN (A)	23.23	10.44	0.0566	25.48	9.53	0.0573	26.36	7.12	0.0557
MMKNN (T)	23.23	10.45	0.0528	25.50	9.56	0.0555	26.32	7.13	0.0528
MMKNN (B)	23.24	10.46	0.0593	25.50	9.56	0.0599	26.31	7.14	0.0588
WMKNN (S)	22.82	10.82	0.0686	25.29	9.97	0.0751	25.66	7.60	0.0757
WMKNN (H)	22.72	10.86	0.0736	25.19	10.00	0.0826	25.45	7.67	0.0814
WMKNN (A)	22.79	10.84	0.0920	25.36	9.92	0.0979	25.68	7.56	0.0944
WMKNN (T)	22.30	11.23	0.0753	24.95	10.46	0.0804	24.88	8.11	0.0775
WMKNN (B)	22.26	11.29	0.0695	24.41	10.40	0.0861	24.79	8.05	0.0838

Table 2. PSNR in dB, MAE, and Processing time values for different images corrupted by 20% of impulsive noise obtained by different filters.

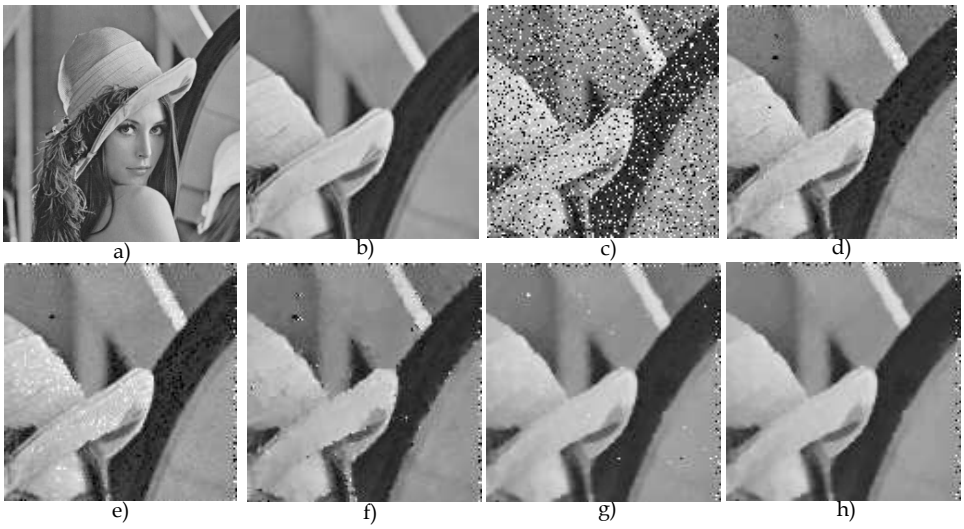

Fig. 3. Subjective visual qualities of a part of image "Lena", a) Original image, b) Zoomed-in section (upright) of (a), c) Degraded image with 20% of impulsive noise of (b), d) Restored image with the ACWM filter of (b), e) Restored image with the ROM filter of (b), f) Restored image with the LMMSE filter of (b), g) Restored image with the MMKNN (H) filter of (b), h) Restored image with the MM-KNN (B) filter of (b).

Table 3 shows the performance results in the grayscale image "Peppers" degraded with 20% of impulsive noise. We observe that the processing time values of ABSTMKNN and MOODMKNN filters are larger than the most comparison filters but the proposed filters consistently outperform other filters by balancing the tradeoff between noise suppression and detail preservation. Figure 4 depicts that the restored image by ABSTMKNN method appears to have a very good subjective quality in comparison with other methods.

Algorithm	PSNR dB	MAE	TIME
KNN	18.83	24.32	0.021380
ABST	22.61	11.10	0.038395
WM	24.68	7.81	0.020341
ACWM	25.18	9.21	0.229951
ROM	25.04	9.62	0.075008
MMEM	24.40	9.67	0.040618
LMMSE	24.75	9.70	0.075140
ABSTMKNN (S)	25.85	7.55	0.063876
ABSTMKNN (H)	25.62	7.75	0.063787
ABSTMKNN (A)	25.95	7.57	0.074301
ABSTMKNN (T)	25.51	7.75	0.063151
ABSTMKNN (B)	25.46	7.75	0.067383
MOODMKNN (S)	25.98	7.55	0.066725
MOODMKNN (H)	25.62	7.75	0.067295
MOODMKNN (A)	25.98	7.57	0.076487
MOODMKNN (T)	25.67	7.64	0.068421
MOODMKNN (B)	25.58	7.66	0.067413

Table 3. Performance results for image "Peppers".

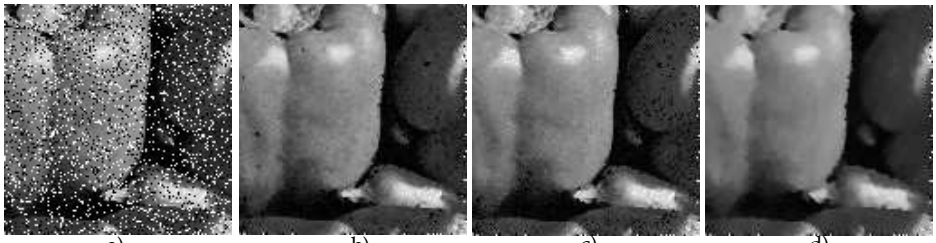

a) b) c) d)

Fig. 4. Results for a part of "Peppers" image, a) Degraded image with 20% of impulse noise, b) Restored image by ACWM filter, c) Restored image by the ROM filter, d) Restored image by the ABSTM-KNN (S) filter.

The MML filter was implemented with Laplacian (L) and Uniform (U) distribution functions, and with (D) and without (ND) impulsive noise detector. Table 1 shows the performance results for "Lena" image degraded with 5% of impulsive noise and σ^2=0.05 of speckle noise. From Table 4, the proposed filter provides better noise suppression and detail preservation than other filters in the most of cases. The processing time of MML filter is less than filters used as comparative, and it takes less time when the impulsive noise detector is

used. Figure 5 exhibits the filtered images in the case of 20% of impulsive noise. The restored image by proposed MML filter appears to have good subjective quality.
To demonstrate the performances of the proposed MML filtering scheme we apply it for filtering of the SAR images, which naturally have speckle noise. The results of such a filtering are presented in the Figure 6 in the case of the image "Pentagon". It is possible to see analyzing the filtering images that speckle noise can be efficiently suppressed, while the sharpness and fine feature are preserved using the proposed filter in comparison with other filters proposed in the references.

Filters	Impulsive noise = 5%			Speckle noise = 0.05		
	PSNR	MAE	TIME	PSNR	MAE	TIME
ACWM	27.73	7.35	0.2299	19.96	20.34	0.2299
ROM	27.49	7.64	0.1050	22.82	20.96	0.1050
MFrost	23.87	12.69	0.1004	24.56	10.99	0.1004
NLMS-L	24.24	11.57	0.1835	21.59	21.54	0.1835
SFWO (L)	24.94	8.38	0.1310	22.10	14.37	0.1310
SFWO (U)	15.76	32.04	0.1310	22.53	12.84	0.1310
MML (A,L,ND)	27.01	7.61	0.0815	22.78	14.21	0.0815
MML (A,U,ND)	28.03	6.13	0.0815	24.61	10.92	0.0815
MML (T,L,ND)	26.93	7.62	0.0796	22.63	14.44	0.0796
MML (T,U,ND)	28.29	5.76	0.0796	24.79	10.63	0.0796
MML (H,L,ND)	27.37	6.92	0.0804	23.12	13.53	0.0804
MML (H,U,ND)	28.40	5.56	0.0804	24.86	10.53	0.0804
MML (A,L,D)	28.62	6.01	0.0684	23.38	13.10	0.0685
MML (A,U,D)	29.10	5.51	0.0684	24.60	11.00	0.0684
MML (T,L,D)	28.59	6.04	0.0652	23.40	13.03	0.0652
MML (T,U,D)	29.23	5.34	0.0651	24.63	10.96	0.0652
MML (H,L,D)	28.75	5.83	0.0790	23.61	12.67	0.0790
MML (H,U,D)	29.33	5.16	0.0790	24.86	10.53	0.0790

Table 4. Performance results in image "Lena" obtained by different filters,

a) b) c) d)

Fig. 5. Filtered images with 20% of impulsive noise: a) Degraded image, b) ACWM, c) ROM, d) MML (A,L,ND).

Table 5 shows the performance results in terms of PSNR in dB and MAE for the image "Lena" degraded with 0.1 of variance of speckle noise and free of noise by use the WDMML

(S,ND,L) filter in approaches (A) and details (D) with the wavelets db1, db2, db3, and db4 with one (1) and two (2) levels of decomposition. From this Table one can see that the proposed WDMML filter provides better speckle noise suppression and detail preservation in comparison with the MML filter in the spatial domain in the most of cases. Figure 7 presents the visual results to apply the proposed filter with one and two decomposition levels in the image "Peppers". One can see from Figure 7 that the proposed WDMML filter outperforms the MML filter in the case of speckle noise.

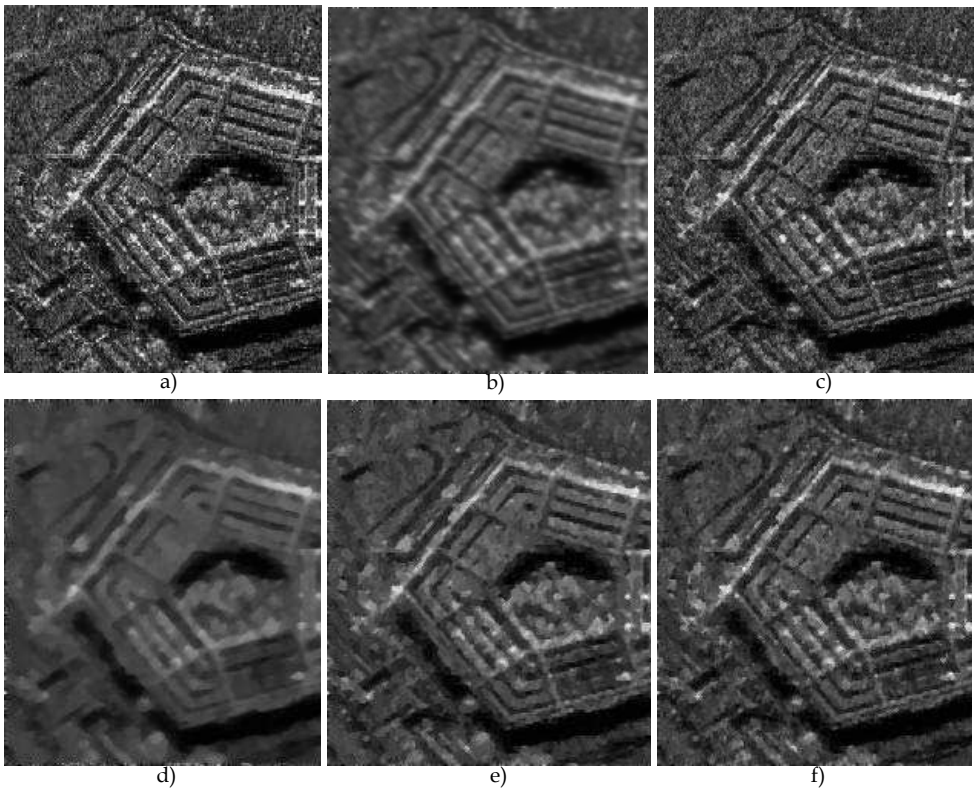

Fig. 6. Comparative results of despeckled SAR image. a) Original image "Pentagon", resolution 1m, source Sandia National Lab., b) Despeckled image with MFrost filter, c) Despeckled image with the ROM filter, d) Despeckled image with the SFWO filter, e) Despeckled image with the MML filter (S, ND, L), f) Despeckled image with the MML filter (S, D, L)

We also propose to apply the proposed filters to video signals. We process a real video sequence to demonstrate that the proposed method potentially could provide a real-time solution to quality video transmission. We investigate a QCIF (Quarter Common Intermediate Format) video sequence. This picture format uses 176x144 luminance pixels per frame and velocity from 15 to 30 frames per second. In the case of this test we used one frame of the video sequence "carphone", that was corrupted by 20% of impulsive noise. The

PSNR, MAE and processing time performances are depicted in Table 6. The restored frames are displayed in Figure 8 by using the ACWM, LMMSE, and MMKNN (H) filters. From the simulation results we observe that the proposed MMKNN and ABSTMKNN filters can process up to 33 frames of QCIF video format suppressing the impulsive noise and providing the detail preservation in real-time applications.

Filters	Free noise		σ^2=0.1	
	PSNR	MAE	PSNR	MAE
MML (S,ND,L)	29.62	3.78	22.95	13.24
WDMML (S,ND,db1,A,1)	27.84	5.09	23.35	12.24
WDMML (S,ND,db1,D,1)	31.46	3.24	20.53	18.78
WDMML (S,ND,db2,A,1)	27.90	5.11	23.60	12.15
WDMML (S,ND,db2,D,1)	32.26	3.05	20.69	18.00
WDMML (S,ND,db3,A,1)	27.92	5.24	24.02	11.77
WDMML (S,ND,db3,D,1)	32.70	2.97	20.79	17.99
WDMML (S,ND,db4,A,1)	27.87	5.27	24.33	11.28
WDMML (S,ND,db4,D,1)	33.00	2.92	20.90	18.11
WDMML (S,ND,db1,A,2)	24.83	8.32	22.46	13.57
WDMML (S,ND,db1,D,2)	27.48	5.73	22.66	13.93
WDMML (S,ND,db2,A,2)	25.40	7.61	22.94	12.85
WDMML (S,ND,db2,D,2)	28.37	5.34	23.21	13.15
WDMML (S,ND,db3,A,2)	25.24	7.89	23.14	12.59
WDMML (S,ND,db3,D,2)	28.39	5.42	23.49	12.90
WDMML (S,ND,db4,A,2)	25.06	8.21	23.38	12.47
WDMML (S,ND,db4,D,2)	28.29	5.46	23.69	12.73

Table 5. Performance results in the image "Lena" obtained by the use of WDMML filter.

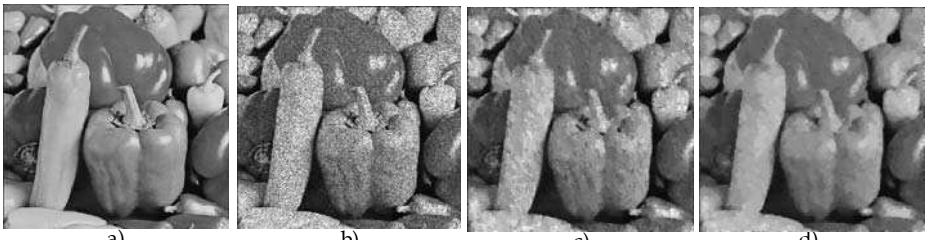

a) b) c) d)

Fig. 7. Visual results in the image Peppers, a) Original image, b) Degraded image with 0.1 of variance of speckle noise, c) Restored image with MML (S,L,ND) filter, d) Restored image with WDMML filter (S,L,ND,db2,A,1).

4.2 Noise suppression in color images and video sequences

The proposed MMKNN, WMKNN, and ABSTMKNN filters were adapted to work in color image and video processing. Now, the proposed Vector RMKNN filters are called as VMMKNN, VWMKNN, and VABSTMKNN filters. These filters have been evaluated, and their performances have been compared with *vector median* (VMF) (Plataniotis &

Algorithm	"Carphone" Frame		
	PSNR	MAE	Time
WM	23.83	9.80	0.009977
TSM	21.53	13.24	0.023730
ACWM	24.34	9.79	0.093865
MMEM	23.60	11.11	0.018021
LMMSE	24.15	10.04	0.034716
MMKNN (S)	24.77	9.08	0.023773
MMKNN (H)	24.76	9.10	0.024018
MMKNN (A)	24.75	9.06	0.025717
MMKNN (T)	24.74	9.16	0.024166
MMKNN (B)	24.78	9.15	0.026760
ABSTMKNN (S)	25.07	9.44	0.027068
ABSTMKNN (H)	24.79	9.66	0.027932
ABSTMKNN (A)	25.08	9.48	0.029762
ABSTMKNN (T)	24.78	9.62	0.026815
ABSTMKNN (B)	24.88	9.62	0.028440

Table 6. PSNR values in dB, MAE, and processing time for different filters in a frame of video sequence "Carphone".

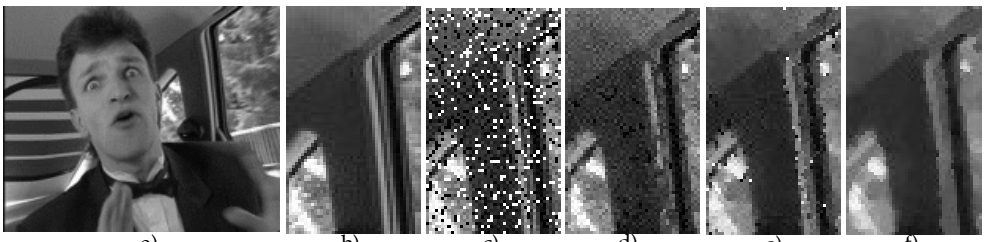

Fig. 8. Subjective visual qualities of a restored frame "Carphone" produced by different filters, a) Original frame, b) Zoomed-in section (upright) of (a), c) Degraded frame with 20% of impulsive noise of (b), d) Restored frame with the ACWM filter of (b), e) Restored frame with the LMMSE filter of (b), f) Restored frame with the MMKNN (H) filter of (b).

Venetsanopoulos, 2000), *α-trimmed mean* (α-TMF), *basic vector directional* (BVDF), *generalized vector directional* (GVDF), *adaptive* GVDF (AGVDF), *double window* GVDF (GVDF_DW), and *multiple non-parametric* (MAMNFE) (Trahanias et al., 1996; Plataniotis et al., 1997) filters.
The implementation of filters were realized on the DSP TMS320C6711 (Kehtarnavaz & Keramat, 2001; Texas Instruments, 1998) to demonstrate that the proposed filters potentially could provide a real-time solution to quality video transmission.
The 320X320 "Lena" color image was corrupted by 20% of impulsive noise. Table 7 shows that the performance criteria are often better for the proposed filters in comparison when other filters are used. Figure 9 exhibits the processed images for test image "Lena" explaining the impulsive noise suppression, and presenting the original image "Lena", image corrupted with noise probability occurrence of 20% for each color channel, and

exhibiting the filtering results produced by the MAMNFE and VMMKNN filters, respectively. The proposed VMMKNN filtering appears to have a better subjective quality in comparison with MAMNFE filtering.

Algorithm	PSNR	MAE	MCRE	NCD	TIME
VMF	21.15	10.73	0.035	0.038	0.039
α-TMF	20.86	14.97	0.046	0.049	0.087
BVDF	20.41	12.72	0.043	0.045	0.065
GVDF	20.67	11.18	0.038	0.040	0.264
AGVDF	22.01	11.18	0.028	0.036	0.620
GVDF_DW	22.59	10.09	0.028	0.039	0.721
MAMNFE	22.67	9.64	0.027	0.035	0.832
VMMKNN (S)	23.15	10.00	0.033	0.034	0.296
VMMKNN (A)	23.07	10.01	0.033	0.035	0.199
VMMKNN (H)	23.05	10.04	0.033	0.035	0.199
VWMKNN (S)	22.99	10.13	0.033	0.035	0.435
VWMKNN (A)	23.00	10.08	0.033	0.035	0.756
VWMKNN (H)	22.99	10.09	0.033	0.035	0.398
VABSTMKNN (S)	22.99	10.13	0.033	0.035	0.286
VABSTMKNN (A)	22.99	10.13	0.033	0.035	0.320
VABSTMKNN (H)	23.01	10.07	0.033	0.035	0.264

Table 7. Comparative restoration results for 20% of impulsive noise for color image "Lena".

a) b) c) d)

Fig. 9. Subjective visual qualities of restored color image "Lena", a) Original test image "Lena", b) Input noisy image with 20% of impulsive noise, c) MAMNFE filtering image, and d) Proposed VMMKNN (S) filtered image.

We use one frame of the video color sequence "Miss America", which was corrupted by 15% of impulsive noise. One can see in Table 8 that the performance criteria are often better for the proposed VMMKNN, VWMKNN, and VABSTMKNN filters in comparison when other filters are used in the most of cases. Figure 10 exhibits the processed frames for test image "Miss America" explaining the impulsive noise suppression. The restored frame with VMMKNN filter appears to have a better subjective quality in comparison with MAMNFE filter that has the better performance among the known color filters.

The processing time performance of the VRMKNN filters depends on the image to process and almost does not vary for different noise levels. These values also depend on the complex calculation of the influence functions and parameters of the proposed filters. From

Tables 7 and 8, one can see that the proposed algorithms can process, in the case of color images of size 320x320 pixels, up to 5 images per second, and in case of QCIF video up to 11 color frames per second in comparison with MAMNFE filter (the best comparative filter) that can process one image per second or 3 frames per second.

Algorithm	PSNR	MAE	MCRE	NCD	TIME
VMF	25.54	5.38	0.0371	0.0332	0.0153
α-TMF	24.47	6.54	0.0589	0.0251	0.0206
BVDF	22.45	7.68	0.0379	0.0329	0.1768
GVDF	23.56	9.12	0.0362	0.0308	0.1869
AGVDF	26.97	5.24	0.0308	0.0302	0.2106
GVDF_DW	26.88	5.95	0.0311	0.0249	0.7205
MAMNFE	27.01	5.82	0.0390	0.0270	0.3219
VMMKNN (S)	28.20	3.86	0.0312	0.0140	0.1109
VMMKNN (A)	28.04	3.91	0.0317	0.0143	0.0898
VMMKNN (H)	28.14	3.90	0.0315	0.0144	0.0917
VWMKNN (S)	27.27	4.48	0.0336	0.0234	0.2662
VWMKNN (A)	26.10	5.10	0.0372	0.0272	0.4599
VWMKNN (H)	26.05	5.05	0.0369	0.0271	0.2912
VABSTMKNN (S)	27.75	4.46	0.0336	0.0243	0.0929
VABSTMKNN (A)	27.56	4.68	0.0349	0.0253	0.2066
VABSTMKNN (H)	27.49	4.71	0.0350	0.0255	0.1194

Table 8. Comparative restoration results for 15% impulsive noise for a color frame of "Miss America"

a) b) c) d)

Fig. 10. Subjective visual qualities of restored color frame "Miss America", a) Original test frame "Miss America", b) Input noisy frame with 15% of impulsive noise, c) MAMNFE filtered frame, and d) Proposed VMMKNN filtered frame (A).

The proposed Wavelet Redundancy of Approaches (WRAF), Wavelet Iterative Center Weighted Median using Redundancy of Approaches (WICWMRAF), Wavelet Signal Dependent Rank-Ordered Mean (WSDROMF), Wavelet Adaptive Center Weighed Median (WACWMF), Wavelet Median M-type K-Nearest Neighbor (WMMKNNF), and Wavelet FIR Median Hybrid (WFIRMHF) Filters were compared with the *Wavelet Iterative Median* (WIMF) and *Wavelet Iterative Center Weighted Median* (WICWMF) (Mahbubur Rahman & Kamrul Hasan, 2003) filters in terms of PSNR, MAE, MCRE and NCD to demonstrate the good quality of color imaging of the proposed filters in both an objective and subjective sense.

Table 9 presents the performance results by means of use different filters in the 512x512 image "Lena" degraded with 20% of impulsive noise and with 0.2 of variance of speckle noise. From these results we observe that the proposed filters provide better impulsive and speckle noise suppression, detail preservation, and color retention in comparison with the traditional filters in the Wavelet domain. Figure 11 shows the subjective visual quantities of a restored zoom part of the color image "Lena" degraded with 0.2 of variance of speckle noise. Figure 12 presents the visual results in a part of "Mandrill" image produced by the WMMKNNF.

Filters	20% of impulsive noise				0.2 of variance of speckle noise			
	PSNR	MAE	MCRE	NCD	PSNR	MAE	MCRE	NCD
WIMF	40.6734	24.7969	0.0172	0.3294	43.7164	22.2675	0.0138	0.2617
WICWMF	40.6734	24.7969	0.0172	0.3294	43.7164	22.2675	0.0138	0.2617
WRAF	44.4936	20.8426	0.0117	0.2718	48.0338	18.2333	0.0093	0.2062
WICWMRAF	50.6952	15.8213	0.0063	0.1911	53.8602	14.1506	0.0056	0.1489
WSDROMF	50.6952	15.8213	0.0063	0.1911	53.8602	14.1506	0.0056	0.1489
WACWMF	50.6952	15.8213	0.0063	0.1911	53.8602	14.1507	0.0056	0.1489
WMMKNNF	50.6953	15.8211	0.0063	0.1911	53.8603	14.1506	0.0056	0.1489
WFIRMHF	50.6992	15.8189	0.0063	0.1911	53.8608	14.1509	0.0056	0.1489

Table 9. Performance results in the image "Lena".

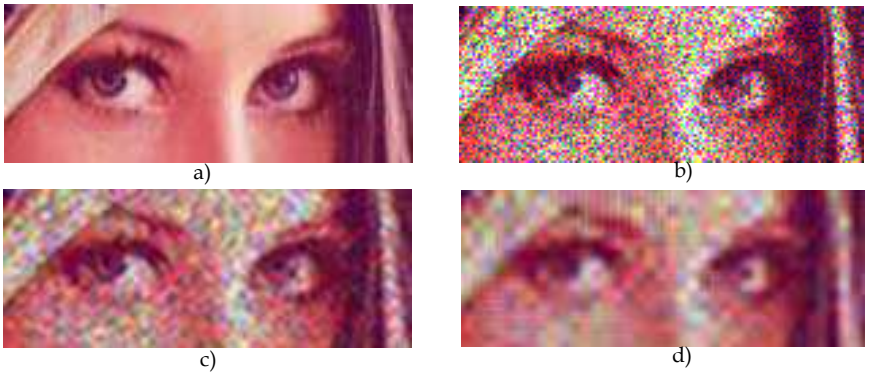

Fig. 11. Subjective visual quantities of restored zoom part of color image "Lena", a) Original image, b) Input noisy image corrupted by 0.2 of variance of speckle noise in each a channel, c) WRAF filtered image; d) WMMKNNF filtered image.

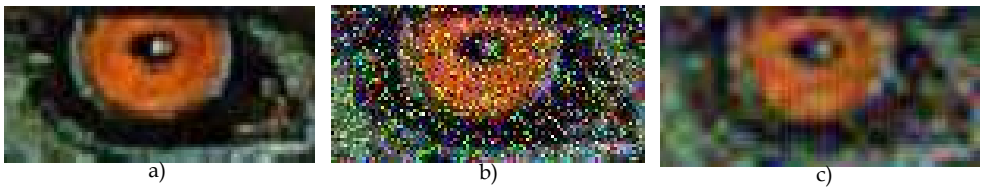

Fig. 12. Subjective visual quantities of restored zoom part of the color image "Mandrill", a) Original image, b) Input noisy image corrupted by 20% impulsive noise in each a channel, c) WMMKNNF filtered image.

4.3 Noise suppression in 3D gray scale video sequences

In this section, we propose 3D filtering algorithms to process ultrasound sequences contaminated by speckle and impulsive noise. The 3D MMKNN and 3D MML filters have been evaluated, and their performance has been compared with different nonlinear 2D filters which were adapted to 3D. The filters used as comparative ones were the *modified a-Trimmed Mean* (MATM), *Ranked-Order* (RO), *Multistage Median* (MSM1 to MSM6), *Comparison and Selection* (CS), *MaxMed*, *Selection Average* (SelAve), *Selection Median* (SelMed), and *Lower-Upper-Middle* (LUM, LUM Sharp, and LUM Smooth) (Astola & Kuosmanen, 1997) filters. These filters were computed according with their references and were adapted to 3D imaging.

An ultrasound sequence of 640x480 pixels with 90 frames (3D image of 640x480x90 voxels) was degraded with 0.05 and 0.1 of variance of speckle noise added to the natural speckle noise of the sequence. The performance results are depicted in Table 10 by use a frame of the sequence. From this Table one can see that the 3D MML filters provide the best results in comparison to other filters proposed as comparative. Figure 13 exhibits the visual results of restored images obtained by the use of different filters according to Table 10. In the Figure we observe that the proposed filters provide the better results in speckle noise suppression and detail preservation in comparison with other filters.

3D Filters	Speckle noise variance			
	0.05		0.1	
	PSNR	MAE	PSNR	MAE
CS	15.435	32.875	13.843	39.778
LUM Smooth	17.915	25.142	15.440	33.823
LUM Sharp	15.625	30.927	14.444	36.425
LUM	15.518	31.427	14.379	36.748
MaxMed	18.562	24.206	15.919	32.913
MATM	20.418	15.124	19.095	18.663
MSM1	20.568	17.624	18.061	23.684
MSM2	20.484	17.789	18.038	23.725
MSM3	22.421	14.206	20.261	18.456
MSM4	21.697	15.401	19.348	20.351
MSM5	19.554	20.207	16.964	27.444
MSM6	22.083	14.688	19.744	19.374
SelAve	21.182	17.647	19.192	22.814
SelMed	20.836	15.750	19.013	20.094
RO	21.587	14.520	19.802	18.179
MMKNN (S)	21.554	15.199	18.949	20.995
MMKNN (H)	21.572	15.169	19.040	20.798
MMKNN (A)	21.399	14.614	18.640	20.226
MMKNN (B)	22.658	13.309	20.075	17.819
MMKNN (T)	22.499	13.446	19.855	18.125
MML (T, U,D)	29.876	5.016	28.6175	5.7429
MML (T, L,D)	28.797	5.646	28.188	6.0194

Table 10. Performance results of different filters in a frame of ultrasound sequence degraded with speckle noise.

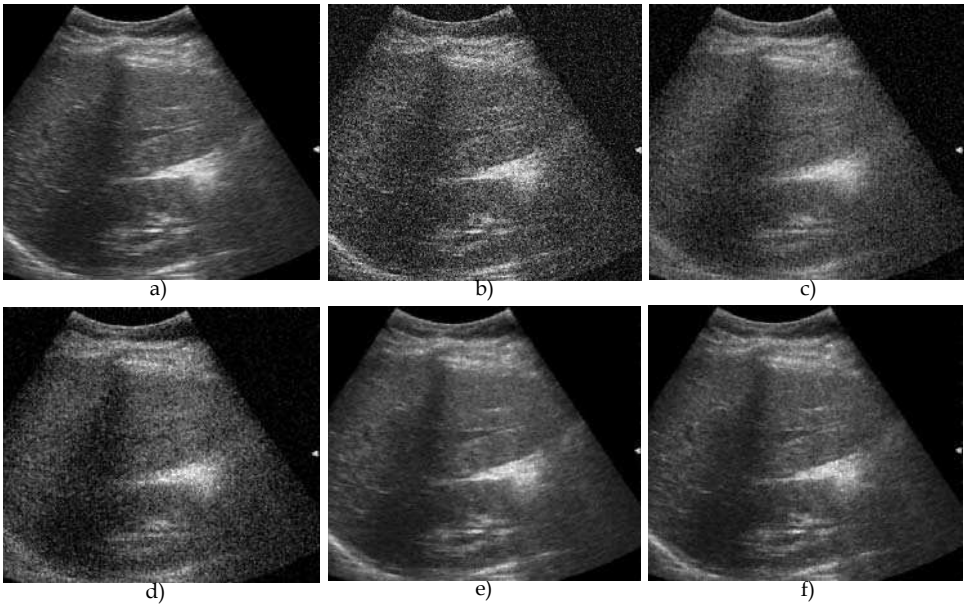

Fig. 13. Visual results in a frame of ultrasound sequence. a) original frame, b) frame degraded by 0.05 of variance of speckle noise, c) restored frame by MSM6 filter, d) restored frame by MMKNN (B) filter, e) restored frame by MML filter (T,U,D), f) restored frame by MML filter (T,L,D).

4.4 Optimal values of parameters of proposed filters

The values of parameters for the RMKNN and MML filters and influence functions were found after numerous simulations with different images and video sequences degraded with different percentages of impulsive noise and variances of speckle noise:

a. Gray scale images and video sequences: The optimal parameters of RMKNN and MML filters are: a=4, K_{min}=5, and K_{max}=8; and s=3 and U=15, respectively. The values for influence functions are: r=25, a=40, and β=200 for *Hampel*, r=35 for *Andrew*, r=15 *Tukey*, and r =20 for *Bernoulli*. Therefore, the WDMML and WMMKNNF filters use the values proposed above.
b. Color images and video sequences: The values of parameters of proposed VRMKNN filters were $0.5<a<12$, K_{min}=5, and K_{max}=8, and the parameters of the influence functions were: $r\leq 81$ for *Andrew*, and α=10, $\beta\leq 90$, and r=300 for *Hampel*.

The processing time performance of the proposed filters depends on the image to process and almost does not vary for different noise levels; these values also depend on the complex calculation of the influence functions and parameters of the proposed filter. The processing time can change with other values for these parameters, increasing or decreasing the times but the PSNR and MAE values change within the range of ±10%, it is due that we fix the parameters to realize the real-time implementation of proposed filters.

5. Conclusions

We present the RMKNN and MML filters in spatial and wavelet domain for impulsive and speckle noise suppression in gray scale and color imaging. Extensive simulation results with different gray scale and color images and video sequences have demonstrated that the proposed filters consistently outperform other filters by balancing the tradeoff between noise suppression, fine detail preservation, color retention, and processing time.

6. References

Abreu, E., Lightstone, M., Mitra, S. K. & Arakawa, K. (1996). A new efficient approach for the removal of impulse noise from highly corrupted images. *IEEE Trans. Image Process.,* Vol.5, No.6, 1012-1025, ISSN:1057-7149

Aizenberg, I., Astola, J., Bregin, T., Butakoff, C., Egiazarian, K., & Paily, D. (2003). Detectors of the Impulsive Noise and new Effective Filters for the Impulsive Noise Reduction, *Proc. SPIE Image Process., Algorithms and Syst. II*, Vol. 5014, ISBN: 9780819448149, pp. 419-428, San Jose, Ca, USA

Astola, J. & Kuosmanen, P. (1997). *Fundamentals of Nonlinear Digital Filtering,* CRC Press. ISBN:0-8493-2570-6, Boca Raton-New York, USA

Bovik, A. (2000). *Handbook of Image and Video Processing,* Academic Press., ISBN:0121197921, San Diego CA

Chen, T., Ma, K. & Chen, L. (1999). Tri-State Median filter for image denoising. *IEEE Trans. Image Process.,* Vol.8, No.12, 1834-1838, ISSN:1057-7149

Chen, T. & Wu, H. R. (2001). Adaptive impulse detection using center-weighted median filters. *IEEE Signal Processing Letters,* Vol.8, No.1, 1-3, ISSN:1070-9908

Gallegos-Funes, F. J., Ponomaryov, V., Sadovnychiy, S., & Nino-de-Rivera, L. (2002). Median M-type K-nearest neighbour (MMKNN) filter to remove impulse noise from corrupted images. *Electron. Lett.*, Vol.38, No.15, 786-787, ISSN:0013-5194

Gallegos, F., & Ponomaryov, V. (2004). Real-time image filtering scheme based on robust estimators in presence of impulsive noise. *Real Time Imaging*, Vol.8, No.2, 78-90, ISSN:1077-2014

Gallegos-Funes, F., Ponomaryov, V., & De-La-Rosa J. (2005). ABST M-type K-nearest neighbor (ABSTM-KNN) for image denoising. *IEICE Trans. Funds. Electronics Comms. Computer Science*, Vol.E88A, No.3, 798-799, ISSN:0916-8508

Gallegos-Funes, F., Varela-Benitez, J., & Ponomaryov, V. (2008). Rank M-Type L (RM L)-Filter for Image Denoising, *IEICE Trans. Funds. Electronics, Comms. Computer Sciences*, Vol.E91A, No.12, 3817-3819, ISSN:0916-8508

Gallegos-Funes, F. J., Martínez-Valdes, J., & De-la-Rosa-Vázquez, J. M. (2007). Order statistics filters in wavelet domain for color image processing, *Proc. IEEE Sixth Mexican Int. Conference on Artificial Intelligence,* ISBN:978-0-7695-3124-3, pp.121-130, Mexico

Huber, P.J. (1981). *Robust Statistics,* Wiley, ISBN:0-471-65072-2, New York, USA

Hampel, F. R., Ronchetti, E. M., Rouseew, P. J. & Stahel, W. A. (1986). *Robust Statistics. The approach based on influence function.* Wiley ISBN:0-471-73577-9, New York, USA

Kehtarnavaz, N., & Keramat, M. (2001). *DSP System Design using the TMS320C6000*, Prentice Hall, ISBN:0-13-091031-7, Upper Saddle River, NJ, USA.

Kotropoulos, C., & Pitas, I. (1996). Adaptive LMS *L*-filters for noise suppression in images. *IEEE Trans. Image Process.*, Vol.5, No.12, 1596-1609, ISSN:1057-7149

Kotropoulos, C. & Pitas, I. (2001). *Nonlinear Model-Based Image/Video Processing and Analysis*, John Wiley & Sons, ISBN:0-471-37735-X, New York

Lukin, V., Melnik, V., Chemerovsky, V., Astola, J., Saarinen, K. (1998). Hard-switching adaptive filter for speckle image processing, *Proc. SPIE Mathematical Modeling and Estimation Techniques in Computer Vision*, Vol. 3457, pp. 31-42, San Diego, USA

Mahbubur Rahman, S. M., & Kamrul Hasan, Md. (2003). Wavelet-domain iterative center weighted median filter for image denoising. *Signal Processing*, Vol.83, No.5, 1001-1012, ISSN:0165-1684

Nikolaidis, N., & Pitas, I. (2001). *3-D Image Processing Algorithms*, John Wiley & Sons, ISBN:0-471-37736-8, New York, USA

Öten, R., De Figueiredo, R.J.P. (2002). Sampled-Function Weighted Order Filters. *IEEE Trans. Circuits and Systems-II,* Vol.49, No.1, 1-10, ISSN:1057-7130

Özkan, M. K., Sezan, M. I. & Murat, A. (1993). Adaptive motion-compensated filtering of noisy image sequences. *IEEE Trans. Circuits and Syst. for Video Tech.*, Vol.3, No.4, 277-290, ISSN:1051-8215

Peltonen, S. & Kuosmanen, P. (2001). Robustness of nonlinear filters for image processing. *J. Electronic Imaging,* Vol.10, No.3, 744-756, ISSN:1560-229X

Plataniotis, K. N., Androutsos, D., Vinayagamoorthy, S. & Venetsanopoulos, A. N. (1997). Color image processing using adaptive multichannel filters. *IEEE Trans. Image Process.*, Vol.6, No.7, 933-949,. ISSN:1057-7149

Plataniotis, K. N., & Venetsanopoulos, A. N. (2000). *Color Image Processing and Applications*, Springer-Verlag, Berlin Heidelberg, ISBN:3-540-66953-1

Ponomaryov, V., Gallegos-Funes, F., Rosales-Silva, A. (2005). Real-Time Color Image Processing Using Order Statistics Filters. *Journal of Mathematical Imaging and Vision,* Vol. 23, No. 3, 315–319, ISSN:0924-9907

Texas Instruments (1998). *TMS320C62x/67x Programmer's Guide, SPRU198D,* Texas Instruments Incorporated. Dallas, USA

Trahanias, P. E., Karakos, D. G., & Venetsanopoulos, A. N. (1996). Directional processing of color images: Theory and experimental results. *IEEE Trans. Image Process.*, Vol.5, No.6, 868-880, ISSN:1057-7149

Varela-Benítez, J. L., Gallegos-Funes, F. J., & Ponomaryov, V. I. (2007a). Real-time speckle and impulsive noise suppression in 3-D imaging based on robust linear combinations of order statistics, *Proc. SPIE Real-Time Image Processing 2007*, Vol.6496, ISBN:9780819466099, pp. 64960H, San Jose, USA

Varela-Benitez, J. L., Gallegos-Funes, F., Ponomaryov, V., De la Rosa Vazquez, J. M. (2007b). RM L-filters in wavelet domain for image processing applications, *Proc. IEEE Sixth Mexican Int. Conference on Artificial Intelligence,* ISBN:978-0-7695-3124-3, pp.113-120, Mexico.

Walker, J. S. (1999). *A Primer on Wavelets and their Scientific Applications*, Chapman & Hall/CRC, ISSN:0-8493-8276-9, Boca Raton-New York, USA

Wei-Yu, H. & Ja-Chen, L. (1997). Minimum-maximum exclusive mean (MMEM) filter to remove impulse noise from highly corrupted images. *Electronics Letters,* Vol.33, No.2, 124-125, ISSN:0013-5194

Image Processing

Edited by Yung-Sheng Chen

ISBN 978-953-307-026-1
Hard cover, 516 pages
Publisher InTech
Published online 01, December, 2009
Published in print edition December, 2009

There are six sections in this book. The first section presents basic image processing techniques, such as image acquisition, storage, retrieval, transformation, filtering, and parallel computing. Then, some applications, such as road sign recognition, air quality monitoring, remote sensed image analysis, and diagnosis of industrial parts are considered. Subsequently, the application of image processing for the special eye examination and a newly three-dimensional digital camera are introduced. On the other hand, the section of medical imaging will show the applications of nuclear imaging, ultrasound imaging, and biology. The section of neural fuzzy presents the topics of image recognition, self-learning, image restoration, as well as evolutionary. The final section will show how to implement the hardware design based on the SoC or FPGA to accelerate image processing.

InTech Europe
University Campus STeP Ri
Slavka Krautzeka 83/A
51000 Rijeka, Croatia
Phone: +385 (51) 770 447
Fax: +385 (51) 686 166
www.intechopen.com

InTech China
Unit 405, Office Block, Hotel Equatorial Shanghai
No.65, Yan An Road (West), Shanghai, 200040, China
中国上海市延安西路65号上海国际贵都大饭店办公楼405单元
Phone: +86-21-62489820
Fax: +86-21-62489821